

FAST RADIO BURSTS: COLLISIONS BETWEEN NEUTRON STARS AND ASTEROIDS/COMETS

J. J. Geng^{1,2}, and Y. F. Huang^{1,2}

ABSTRACT

Fast radio bursts (FRBs) are newly discovered radio transient sources. Their high dispersion measures indicate an extragalactic origin. But due to the lack of observational data in other wavelengths, their progenitors still remain unclear. Here we suggest the collisions between neutron stars and asteroids/comets as a promising mechanism for FRBs. During the impact process, a hot plasma fireball will form after the material of the small body penetrates into the neutron star surface. The ionized matter inside the fireball will then expand along the magnetic field lines. Coherent radiation from the thin shell at the top of the fireball will account for the observed FRBs. Our scenario can reasonably explain the main features of FRBs, such as their durations, luminosities, and the event rate. We argue that for a single neutron star, FRBs are not likely to happen repeatedly in a foreseeable time span since such impacts are of low probability. We predict that faint remnant X-ray emissions should be associated with FRBs, but it may be too faint to be detected by detectors at work.

Subject headings: pulsars: general — radio continuum: general — stars: neutron — minor planets, asteroids: general

1. INTRODUCTION

Recently, the discovery of a number of fast radio bursts (FRBs) was reported (Lorimer et al. 2007; Keane et al. 2011; Thornton et al. 2013; Burke-Spolaor & Bannister 2014; Spitler

¹School of Astronomy and Space Science, Nanjing University, Nanjing 210046, China; hyf@nju.edu.cn

²Key Laboratory of Modern Astronomy and Astrophysics (Nanjing University), Ministry of Education, Nanjing 210046, China

et al. 2014; Ravi et al. 2015). Typically, they are single radio pulses with flux densities $S_\nu \sim$ a few Jy and durations $\delta t \sim$ a few ms at frequency $\nu_{\text{FRB}} \sim 1$ GHz. No counterparts in other wavelengths have been detected yet (Petroff et al. 2015), maybe due to the lack of rapid, multiwavelength follow-up after the bursts. According to their high dispersion measures ($\sim 500 - 1000 \text{ cm}^{-3} \text{ pc}$), FRBs may originate at cosmological distances (Thornton et al. 2013), although the possibility that they happened in the dense regions of local galaxies still cannot be excluded yet (Katz 2014b; Luan & Goldreich 2014; Pen & Connor 2015). If FRBs are at cosmological distances with redshifts $0.5 \leq z \leq 1$ (Thornton et al. 2013), the characteristic isotropic radio luminosity (L_{FRB}) will be $\sim 10^{42-43} \text{ erg s}^{-1}$ and the isotropic energy (E_{FRB}) released is then 10^{39-40} erg . The observable event rate of FRBs is suggested to be $\sim 10^4 \text{ sky}^{-1} \text{ day}^{-1}$ (Thornton et al. 2013; Keane & Petroff 2015).

The central engines of FRBs are under hot debate. The durations of FRBs indicate the emission regions are compact, while the high brightness of the radio emission requires coherent emission to take effect (Katz 2014a; Luan & Goldreich 2014), which is similar to radio emissions from pulsar magnetospheres (Ruderman & Sutherland 1975; Cheng & Ruderman 1977; Benford & Buschauer 1977). Also, the energy reservoir in a neutron star (NS) magnetosphere is high enough to account for the energy release of FRBs. These few but significant clues motivate some authors to associate FRBs with scenarios involving NSs. Several possible models have been proposed, e.g., magnetar giant flares (Popov & Postnov 2007; Kulkarni et al. 2014; Lyubarsky 2014; Pen & Connor 2015), collapse of hypermassive neutron stars (NSs) into black holes (Falcke & Rezzolla 2014; Zhang 2014; Ravi & Lasky 2014), binary NS mergers (Totani 2013) and planetary companions around NSs (Mottez & Zarka 2014). At the same time, other kinds of models have also been proposed, e.g., binary white dwarf mergers (Kashiyama et al. 2013), flare stars (Loeb et al. 2014) and evaporation of primordial black holes (Barrau et al. 2014).

However, besides the above scenarios, there may be another external way to trigger the energy release in the NS magnetosphere. Pulsar timing observations have revealed that there may be planets (Wolszczan & Frail 1992) or asteroid belts (Shannon et al. 2013) around NSs. Recent study shows transient, supergiant pulses from active or dormant pulsars may be triggered by debris entering their magnetospheres (Cordes & Wasserman 2015). By migrating into the NS light cylinder before completely destroyed by evaporation and ionizing,

the debris can also disrupt current flows and electromagnetic radiation and therefore account for some intermittency seen in pulsars (Cordes & Shannon 2008). On the other hand, it has previously been suggested in the literature that small solid bodies such as asteroids or comets can impact NSs occasionally (Colgate & Petschek 1981; Mitrofanov & Sagdeev 1990; Katz et al. 1994; Huang & Geng 2014). By referring to impact, we mean we are considering small bodies of ballistic trajectories (with low angular momentum), as apposed to orbiting objects with significant angular momentum. It is interesting to notice that the timescale and energy release of these impacts can meet the requirements of FRB progenitors from the first view. Thus we suggest that the impacts between NSs and comets/asteroids may provide a possible explanation for FRBs.

The structure of our paper is as follows. We briefly describe the impact process in Section 2. In Section 3, we present the formulas for the radiation process and derive the basic features of the emission. In Section 4, the remnant X-ray emission in our scenario is discussed. Our conclusions are summarized in Section 5.

2. IMPACT PROCESS

In our modeling, the calculations are mainly based on the assumption that FRBs are at cosmological distances with redshifts $0.5 \leq z \leq 1$. The absence of correlation of FRBs with any known galaxies or galaxy clusters indicates a lower bound on their distance (~ 100 Mpc, Katz (2014b)). Note that if FRBs happen at such a local distance, our model can still work. In that case, we will only need a smaller asteroid to collide with the NS. A more detailed discussion on this point is given in the last section of our paper.

Direct impacts between asteroids/comets and NSs have been previously discussed in different contexts. In order to give a quantitative description of our model, here we would like to give a brief review of the impact process, mainly following the study in Colgate & Petschek (1981). When a small solid body of mass m falls freely in the gravitational field of an isolated NS of mass M , it will undergo elongation in the radial direction. The elongated body will be broken up at the breakup radius and the collapsed material will be compressed by gravitational radial acceleration and magnetic fields of the NS before landing. For an Fe-Ni asteroid with a density ρ_0 , radius r_0 , and shear strength s , the breakup radius of the

elongated body is

$$R_b = (\rho_0 r_0^2 M G / s)^{1/3}, \quad (1)$$

where G is the gravitational constant. We assume the leading fragment (at $R_b - r_0$) and lagging portion (at $R_b + r_0$) have the same velocity v_b (v_b is determined from the free fall assumption from $R = \infty$) when the asteroid center is at R_b . The subsequent free fall gives the evolution of the velocities of the leading and lagging fragments (v_- and v_+) as

$$\frac{1}{v_{\pm}} \approx \left(\frac{2GM}{R} \right)^{-1/2} \left(1 \pm \frac{r_0 R}{2R_b^2} \right). \quad (2)$$

The difference of arrival time at the surface of the NS (R_{NS}) is then

$$\begin{aligned} \Delta t_a &= \int_{R_{\text{NS}}}^{R_b+r_0} \frac{dR}{v_+} - \int_{R_{\text{NS}}}^{R_b-r_0} \frac{dR}{v_-} \simeq 2r_0/v_b = 2r_0 \left(\frac{2GM}{R_b} \right)^{-1/2} \\ &= 1.58 \times 10^{-3} m_{18}^{4/9} s_{10}^{-1/6} \left(\frac{\rho_0}{8 \text{ g cm}^{-3}} \right)^{-5/18} \left(\frac{M}{1.4 M_{\odot}} \right)^{-1/3} \text{ s}, \end{aligned} \quad (3)$$

where the convention $Q_x = Q/10^x$ in cgs units is adopted hereafter. This impact time scale is less than the duration of the observed FRBs, so the short-time characteristic of FRBs can basically be met in our model.

The descriptions above only consider the gravitational influence of the NS on a potential impacting body. In realistic case, as the asteroid moves toward the NS, it may be evaporated and ionized by radiation from the compact star and its magnetosphere before impacting the NS (Cordes & Shannon 2008). Note that in our model, the conditions are somewhat special. First, the asteroids are of low angular momentum and possess ballistic trajectories, as opposed to orbiting objects that are spiraling in. Second, the mass of the asteroid is relatively large (typically $\sim 10^{18}$ g, see Section 3 below). It is much larger than the characteristic mass discussed by Cordes & Shannon (2008) for which the effects of evaporation and ionization are important. Third, the asteroid is assumed to be of Fe-Ni composition and the shear strength will be larger. As a result, the asteroid might be less prominently affected by factors other than the gravitational influence. We now present a detailed discussion on this point.

For slowly spinning old pulsars, ionization does not happen until the asteroid has entered the magnetosphere. The luminosity of X-rays from the magnetosphere may not be high if the tilt angle of the dipolar magnetic field is small (Cordes & Shannon 2008) so that we only need

to consider the radiation from the NS surface here. For an old NS with a surface temperature of T_{NS} , assuming that the asteroid at R is in thermal equilibrium with the NS surface radiation, then the temperature of the asteroid is $T_* = T_{\text{NS}} (R_{\text{NS}}/2R)^{1/2} \simeq 707 T_{\text{NS},5} R_{10}^{-1/2}$ K. When T_* reaches the iron evaporation point ($\simeq 2000$ K), the corresponding distance is smaller than typical R_b ($\simeq 2 \times 10^9$ cm). It means the evaporation process could be ignored before the tidal breakup. We now consider possible electrodynamic effects imposed by the magnetosphere. After the accreted matter enters the magnetosphere, it will be conducting because of the immense electric field in the frame of the matter. The magnetic skin depth will be small ($\sim 10^{-2}$ cm) since the conductivity is large (Colgate & Petschek 1981). Therefore, when the accretion column penetrates between two surfaces of constant longitude, it can be treated as a diamagnetic body with all field lines parallel to its surface. On the other hand, if the accretion column crosses some regions with a nonzero field-aligned electric field ($E_{\parallel} \neq 0$, e.g., Takata et al. (2006)), particle acceleration in these regions can yield γ -ray emission that drives electron/positron pair cascades. With these free charges, E_{\parallel} of these regions may actually turn to be zero since the magnetosphere tends to become force-free. As a result, in our model, E_{\parallel} may not have a strong influence on the trajectory of the main part of the incoming matter at the expense of a little front intruding matter. Thus the result of Equation (3) will not be seriously affected after considering the effects of the NS magnetic field in our framework.

When approaching the NS surface, the accretion column will penetrate the magnetic field as a compressed sheet of diamagnetic fluid with all magnetic field lines parallel to its surface. The compression in longitude reduces the thickness of the sheet to a few millimeters, while its width in latitude would expand to a few kilometers at the NS surface. The dense matter then plunges into the NS outer crust and the kinetic energy is converted to thermal energy, launching a rapidly expanding plasmoid fireball along the field lines (see Figure 1 for a schematic illustration). A fan of field lines is finally filled with hot plasma (Tademaru 1971; Colgate & Petschek 1981). In the plasma, plenty of electrons are accelerated to ultra-relativistic speeds by magnetic reconnection near the collision site. Radiation from this fan of hot plasma will give birth to an observable FRB, as detailed in the following section.

3. EMISSION MECHANISM

The high brightness temperatures of FRBs indicate they are connected with coherent emission. This radiation mechanism may also be involved in radio emission of pulsars. Although the progenitors of FRBs are still uncertain, some constraints on the emission region can be derived from observations (Katz 2014b). In our scenario, the hot plasma fan can produce the required coherent emission (see Figure 1). The electron bunches originated from the collision will form a shell with a thickness of Δ at r_{emi} from the NS. The duration δt of FRBs implies $\Delta \approx c\delta t$. The emission volume of this shell is $V_{\text{emi}} \approx 4\pi f\Delta r_{\text{emi}}^2$. Note that f is the ratio of the shell solid angle to 4π . At the bottom of the fan, the thickness in longitude is $\sim 10^4$ cm as a result of the turbulent expansion, thus a rough estimate gives $f \sim \frac{10^4 \text{ cm}}{2\pi R_{\text{NS}}} = 3 \times 10^{-3}$. Electrons radiate coherently in patches with a characteristic radial size of $\lambda = c/\nu_c$ (ν_c is the characteristic frequency of curvature emission), the corresponding volume of each patch is $V_{\text{coh}} = (4/\gamma^2) r_{\text{emi}}^2 \times (c/\nu_c)$. Here the factor $4/\gamma^2$ is the solid angle within which electrons can be casually connected in the relativistic beam.

The coherent curvature emission luminosity can be estimated as (Kashiyama et al. 2013)

$$L_{\text{tot}} \approx (P_e N_{\text{coh}}^2) \times N_{\text{pat}}, \quad (4)$$

where $P_e = 2\gamma^4 e^2 c / 3r_{\text{emi}}^2$ is the emission power of a single electron, $N_{\text{coh}} \approx n_e \times V_{\text{coh}}$ is the number of electrons in each coherent patch, and $N_{\text{pat}} \approx V_{\text{emi}}/V_{\text{coh}}$ is the number of the patches. The characteristic frequency of curvature emission is

$$\nu_c = \gamma^3 \frac{3c}{4\pi r_{\text{emi}}}. \quad (5)$$

On the other hand, the coherent radiation mechanism may be effective only within a certain distance r_{max} from the pulsar, since the filamentary instability would grow beyond r_{max} (Benford & Buschauer 1977). Above r_{max} , the transverse pressure of plasma begins to exceed the magnetic energy density and the coherent emission vanishes (Benford & Buschauer 1977). As r_{emi} may be slightly less than r_{max} , we introduce a parameter ϵ to describe the deviation from the balance between the plasma pressure and the magnetic energy density, i.e. $n_e \gamma m_e c^2 = \epsilon B^2(r_{\text{emi}})/8\pi$. Here the magnetic field strength can be estimated as $B(r_{\text{emi}}) \approx B_{\text{NS}} \times (r_{\text{emi}}/R_{\text{NS}})^{-3}$, where B_{NS} is the surface magnetic field strength at R_{NS} .

Using the formulas above and assuming $L_{\text{tot}} = fL_{\text{FRB}}$, $\nu_c = \nu_{\text{FRB}}$, we can solve out the typical Lorentz factor of electrons in the emitting shell as

$$\gamma \simeq 547 \left(\epsilon_0^2 B_{\text{NS},12}^4 R_{\text{NS},6}^{12} \delta t_{-2} \nu_{\text{FRB},9}^9 L_{\text{FRB},42}^{-1} \right)^{1/30}. \quad (6)$$

The corresponding typical values of other quantities are $r_{\text{emi}} \simeq 1.2 \times 10^9$ cm, $\Delta \simeq 3 \times 10^8$ cm, $B(r_{\text{emi}}) \simeq 580$ G, and $n_e \simeq 3 \times 10^7$ cm⁻³. It is worthy to note that n_e actually refers to the number density of electrons and positrons generated from photon pair production. Therefore, it could be significantly larger than the Goldreich-Julian density (Goldreich & Julian 1969). Also, it can be found that γ and other quantities are insensitive to f (or the real emission volume). Actually, the emission volume can be larger than the volume derived from $f \sim 3 \times 10^{-3}$ above.

For the radio emission propagating through the plasma, it is essential that the characteristic plasma frequency must be below the frequency of the propagating radio waves, i.e.,

$$\nu_p = \gamma \left(\frac{n'_e e^2}{\pi m_e} \right)^{1/2} \leq \nu_{\text{FRB}}, \quad (7)$$

where $n'_e = n_e/\gamma$ is the number density of electrons in the comoving frame. Using the parameters derived above, we find this requirement can be satisfied.

In general, both the gravitational potential energy of the asteroid and the magnetic field energy of the NS can provide the energy emitted. If all the energy released is contributed by the former one, i.e.,

$$fE_{\text{FRB}} = \eta_{\text{R}} \frac{GMm}{R_{\text{NS}}}, \quad (8)$$

then the mass needed is $m = 5.4 \times 10^{17} \eta_{\text{R},-2}^{-1} f_{-3} E_{\text{FRB},40} R_{\text{NS},6} M_{1.4M_{\odot}}^{-1}$ g, where η_{R} is the efficiency of transforming the potential energy into radio radiation and we adopt $\eta_{\text{R}} \sim 10^{-2}$ as the typical value in the following calculations. This mass is roughly in the mass range of normal asteroids, assuring the self-consistency of our model.

4. X-RAY EMISSION

No counterparts associated with FRBs have been observed at wavelengths other than the radio range till now, making FRBs more mysterious. A recent multiwavelength follow-

up to FRB 140514 reveals no variable counterparts or transient emissions associated with it (Petroff et al. 2015). There are two possible reasons for this mysterious fact. On one hand, the progenitors of FRBs may be such special transient sources so that the duration of signals in other bands are also too short, beyond the reaction capability of telescopes in search. On the other hand, the flux of FRB counterparts may be very weak and be below the detection limit of the telescopes. In our scenario, the matter collapsed onto the NS surface may contribute to emissions in other bands. It is interesting to discuss whether the remnant emissions can be detected by detectors at work.

While some electrons are accelerated to move to the top of the fan, most of the matter collapsed would remain in a column on the NS surface. The temperature of this matter is high during the impact, and would decrease later when it loses its energy by radiation. Although the cooling process of the hot matter is not clearly known, we can have a rough estimate on the basis of reasonable assumptions. After the giant flare of 1998 August 27, transient X-ray emission decaying as $\propto t^{-0.7}$ was observed from SGR 1900+14. It was suggested to be the cooling behavior of the heated crust of magnetar (Lyubarsky et al. 2002). In our model, we assume that the radiation from the heated matter is thermal and the cooling obeys the same decaying law. Thus, for a FRB at a luminosity distance of d_L , the remnant X-ray light curve is

$$F_X \approx \sigma T^4 \left(\frac{R_{\text{NS}}}{d_L} \right)^2, \quad (9)$$

where σ is the Stefan-Boltzmann constant and T is the temperature of the matter. The $t^{-0.7}$ decaying law indicates that the matter cools as $T \propto t^{-7/40}$. We further assume the ratio of the energy released in X-ray band to the potential energy is η_X . Then we can obtain F_X and compare it with the sensitivity of current detectors. Figure 2 illustrates the X-ray light curves calculated using different η_X (ranging from 10^{-2} to 1.0), together with the sensitivity line of the *Swift*/X-Ray Telescope (Moretti et al. 2009; Burrows et al. 2014; Yi et al. 2014). From this figure, it can be seen that the remnant X-ray emission after the collision is well below the sensitivity line and cannot be detected.

Other factors, e.g., the spreading of the collapsed matter on the NS surface, and the rotation of the NS, would reduce the flux significantly and are not considered here. The calculation above is actually an optimistic estimate. Therefore, the X-ray counterparts (not in the bursting phase) associated with FRBs may not be detected by detectors at work.

5. SUMMARY AND DISCUSSION

In this study, we propose that the impacts between NSs and asteroids/comets may be a promising mechanism for FRBs. For an asteroid of typical mass of 10^{18} g falling onto the NS surface, a fan of hot plasma would form after the millisecond collision. The consequent emitting shell at $r_{\text{emi}} \sim 1.2 \times 10^9$ cm, containing electrons/positrons with $\gamma \approx 550$, will emit in radio wavelength coherently. The main characteristics of FRBs, including the timescale and luminosity, can be well explained in our scenario. However, the remnant X-ray emission following the FRBs will be faint according to the calculations under reasonable assumptions.

In our scenario, γ -ray photons may be emitted, e.g., by the inverse Compton scattering of transient energetic electron/positron pairs on the soft photons within burst timescale. The γ -ray event may be as short as the radio burst itself, but might last for a rotation period or longer. The fraction of electron/positron pairs with a high Lorentz factor to trigger γ -ray emission is highly uncertain, but we can give a rough estimate based on some simplifications. We assume the efficiency of transferring the potential energy into γ -ray emission is η_γ and the duration τ is the same to that of radio burst, i.e., $\tau \sim \delta t \simeq 1$ ms. Then we can find the average γ -ray flux during τ as $\sim \frac{\eta_\gamma}{\eta_{\text{R}}} \frac{f E_{\text{FRB}}}{4\pi d_L^2 \tau} = 10^{-19} f_{-3} \eta_{\gamma,-2} S_{\nu,1\text{Jy}} \nu_{\text{FRB},9} \tau_{-3}^{-1}$ erg cm $^{-2}$ s $^{-1}$, which is too low to detect.

The main calculations in this paper are based on the assumption that the FRBs are generated at cosmological distances. Nevertheless, our scenario can also work for FRBs that somehow happen in local galaxies. For an FRB happens at $d_L \sim 100$ Mpc, its isotropic radio energy is then $\sim 10^{37}$ erg. Using Equation (8), we can find that the corresponding asteroid mass needed is only $\sim 5 \times 10^{15}$ g. Although the distance is much smaller in this case, the remnant X-ray flux is still low since the potential energy (and thus the X-ray energy release) is accordingly reduced. However, note that the dynamics of small objects ($\sim 10^{15}$ g) could be significantly different from that of large objects ($\sim 10^{18}$ g), because the evaporation and electrodynamic effects may be stronger (Cordes & Shannon 2008). A detailed study on these effects will be helpful but it is beyond the scope of this paper.

Till now, no repeating bursts have been observed from any particular FRB sources. This feature can be reasonably explained in our scenario since a direct collision between an asteroid/comet and the NS can only trigger the burst once, and such collisions are not likely

to happen repeatedly on short timescales. These predictions make our model testable by more observations in the future.

The event rate of FRBs is another crucial clue to the progenitors. The very limited field of view of current large radio telescope makes the observation of large numbers of FRBs very difficult. Although only a few FRBs have been observed till now, it is widely believed that the actual event rate should be very high, i.e., $\sim 10^4 \text{ sky}^{-1} \text{ day}^{-1}$ (Keane & Petroff 2015). We need to know whether this event rate could be explained in our framework. Although it is difficult to assess the exact event rate of our impact processes theoretically, we can give a rough estimate on the basis of some reasonable assumptions. Several mechanisms have been proposed for the formation of planetary systems around NSs. The planetary system can be formed along with the progenitor (Wolszczan & Frail 1992; Phinney & Hansen 1993; Podsiadlowski 1993), from the fall back material after the supernova (Lin et al. 1991), or from the material provided by a lower mass companion (Nakamura & Piran 1991; Shannon et al. 2013). For a NS with a planetary system, it is possible that some asteroids would impact the NS. First, asteroids could be gravitationally disturbed by other planets and be scattered toward the NS (Guillochon et al. 2011). Second, the planets may have chances to collide with each other and produce clumps falling to the NS (Katz et al. 1994). In previous studies, the recurrence time (τ_{rec}) of strong direct impacts (with $m \geq 10^{18} \text{ g}$) in a typical NS planetary system is estimated to be $\sim 10^6 - 10^7$ years (Tremaine & Zytkow 1986; Mitrofanov & Sagdeev 1990; Katz et al. 1994; Litwin & Rosner 2001). Noting that the co-moving volume of $z \leq 1$ contains $\sim 10^9$ late-type galaxies (Thornton et al. 2013), and supposing the number of NSs in a typical galaxy is 10^8 (Timmes et al. 1996), the observable event rate of the impact is $\zeta \approx f \frac{10^9 \text{ galaxies} \times 10^8 / \text{galaxy}}{\tau_{\text{rec}}} \simeq 10^4 - 10^5 f_{-3} \text{ sky}^{-1} \text{ day}^{-1}$. Recently the Alfvén wing structures formed during the interaction between a relativistic pulsar wind and the orbiting small body were investigated. It was found that the Alfvén wing structures will lead the small bodies in a retrograde orbit to move toward the central NS more rapidly (Mottez & Heyvaerts 2011), which can further increase the collision rate. Considering these, the theoretical event rate can well explain the observed FRB rate.

By now, what we are confident about is that the radio emission of FRB should be coherent given the millisecond duration and a lower bound on the distance. In fact, what we have proposed is one kind of process that can trigger the coherent emission from the

magnetosphere of NS. The conditions needed to drive the particle bunching, which may involve some kinds of instabilities, is still unclear and is beyond the scope of our work. Future advance in the study of coherent radiation could give more rigorous clues to the progenitors of FRBs.

We appreciate many helpful comments and suggestions from the anonymous referee. We thank Shuang-Xi Yi and Wei Su for helpful discussions. This study was supported by the National Basic Research Program of China with Grant No. 2014CB845800, and by the National Natural Science Foundation of China with Grant No. 11473012.

REFERENCES

- Barrau, A., Rovelli, C., & Vidotto, F. 2014, *Phys. Rev. D*, 90, 127503
- Benford, G., & Buschauer, R. 1977, *MNRAS*, 179, 189
- Burke-Spolaor, S., & Bannister, K. W. 2014, *ApJ*, 792, 19
- Burrows, D. N., Frank, K. A., & Park, S. 2014, *BAAS*, 223, 353.14
- Cheng, A. F., & Ruderman, M. A. 1977, *ApJ*, 212, 800
- Colgate, S. A., & Petschek, A. G. 1981, *ApJ*, 248, 771
- Cordes, J. M., & Shannon, R. M. 2008, *ApJ*, 682, 1152
- Cordes, J. M., & Wasserman, I. 2015, *arXiv:1501.00753*
- Falcke, H., & Rezzolla, L. 2014, *A&A*, 562, A137
- Goldreich, P., & Julian, W. H. 1969, *ApJ*, 157, 869
- Guillochon, J., Ramirez-Ruiz, E., & Lin, D. 2011, *ApJ*, 732, 74
- Huang, Y. F., & Geng, J. J. 2014, *ApJL*, 782, L20
- Kashiyama, K., Ioka, K., & Mészáros, P. 2013, *ApJL*, 776, L39

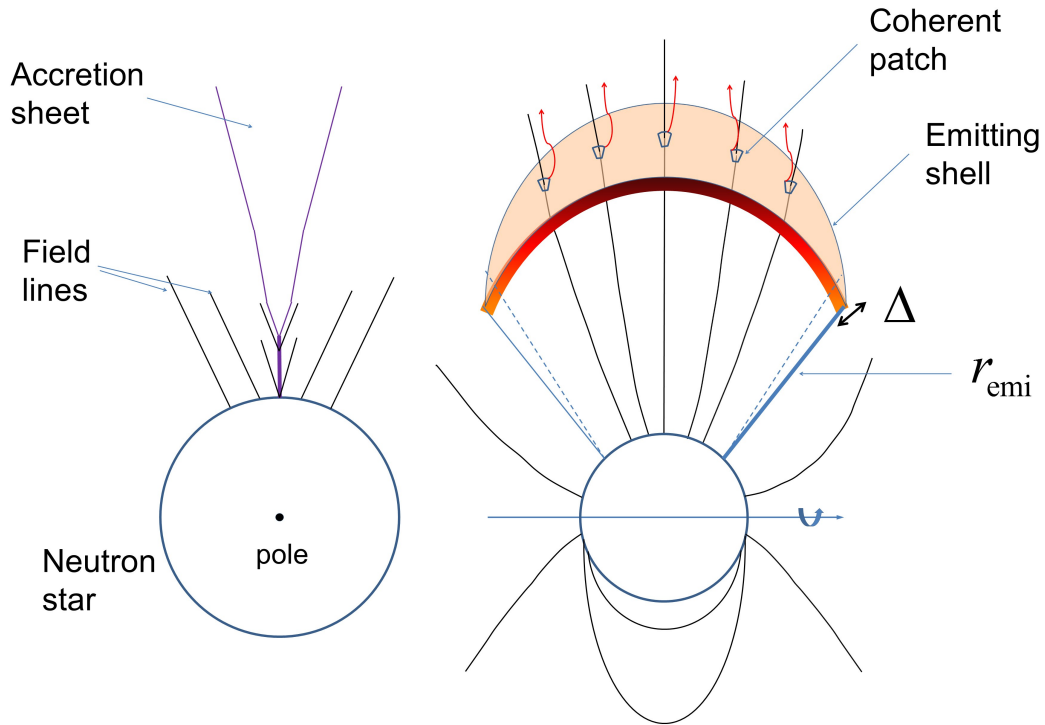


Fig. 1.— Schematic illustration of the impact between a NS and an asteroid/comet. The left panel shows the elongated body is accreted onto the NS as a sheet (see Colgate & Petschek (1981) for a detailed plot). The magnetic compression in longitude reduces its thickness to a few millimeters, while the width in latitude would expand to a few kilometers when approaching the NS surface. The right panel depicts the hot plasma fan generated shortly after the collision. The emitting shell (red-orange arc) is the region where the coherent curvature radiation is generated.

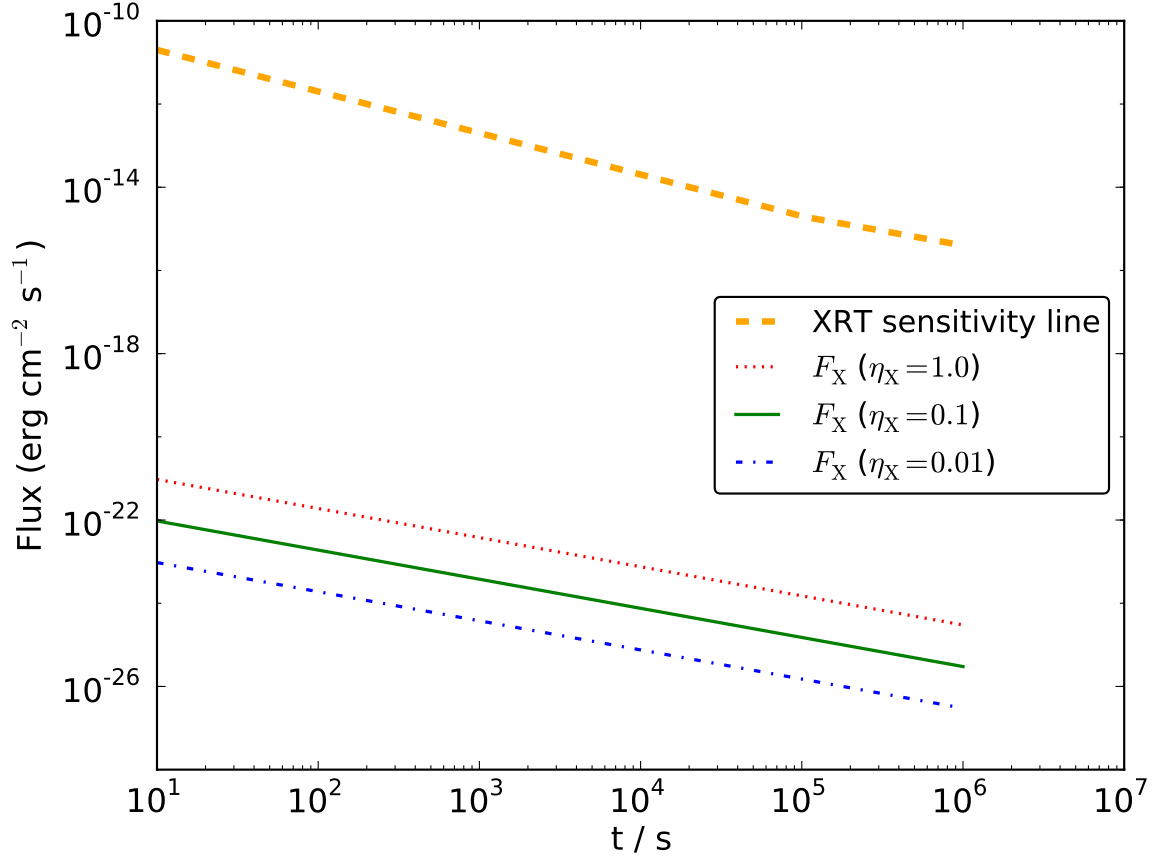


Fig. 2.— Predicted remnant X-ray light curves after the FRBs in our scenario. Three values of $\eta_X = 1.0$ (dotted line), 0.1 (solid line), 0.01 (dash-dotted line) are adopted during the calculation using Equation (9). Other quantities are set as typical values, i.e. $\eta_R = 0.01$, $f = 10^{-3}$, $E_{\text{FRB}} = 10^{40}$ erg. The thick dashed line is the sensitivity line of the *Swift*/X-Ray Telescope (Moretti et al. 2009; Burrows et al. 2014; Yi et al. 2014). Note that for the sensitivity line, the X-axis is the integration time, while the Y-axis is the corresponding sensitivity limit under this exposure time.

- Katz, J. I., Toole, H. A., & Unruh, S. H. 1994, *ApJ*, 437, 727
- Katz, J. I. 2014a, *Phys. Rev. D*, 89, 103009
- Katz, J. I. 2014b, arXiv:1409.5766
- Keane, E. F., Kramer, M., Lyne, A. G., Stappers, B. W., & McLaughlin, M. A. 2011, *MNRAS*, 415, 3065
- Keane, E. F., & Petroff, E. 2015, *MNRAS*, 447, 2852
- Kulkarni, S. R., Ofek, E. O., Neill, J. D., Zheng, Z., & Juric, M. 2014, *ApJ*, 797, 70
- Lin, D. N. C., Woosley, S. E., & Bodenheimer, P. H. 1991, *Nature*, 353, 827
- Litwin, C., & Rosner, R. 2001, *Physical Review Letters*, 86, 4745
- Loeb, A., Shvartzvald, Y., & Maoz, D. 2014, *MNRAS*, 439, L46
- Lorimer, D. R., Bailes, M., McLaughlin, M. A., Narkevic, D. J., & Crawford, F. 2007, *Science*, 318, 777
- Luan, J., & Goldreich, P. 2014, *ApJL*, 785, L26
- Lyubarsky, Y. 2014, *MNRAS*, 442, L9
- Lyubarsky, Y., Eichler, D., & Thompson, C. 2002, *ApJL*, 580, L69
- Mitrofanov, I. G., & Sagdeev, R. Z. 1990, *Nature*, 344, 313
- Moretti, A., Pagani, C., Cusumano, G., et al. 2009, *A&A*, 493, 501
- Mottez, F., & Heyvaerts, J. 2011, *A&A*, 532, A22
- Mottez, F., & Zarka, P. 2014, *A&A*, 569, A86
- Nakamura, T., & Piran, T. 1991, *ApJL*, 382, L81
- Pen, U.-L., & Connor, L. 2015, arXiv:1501.01341
- Petroff, E., Bailes, M., Barr, E. D., et al. 2015, *MNRAS*, 447, 246

- Phinney, E. S., & Hansen, B. M. S. 1993, in ASP Conf. Ser. 36, Planets Around Pulsars, ed. J. A. Phillips, S. E. Thorsett, & S. R. Kulkarni (San Francisco, CA: ASP), 371
- Podsiadlowski, P. 1993, in ASP Conf. Ser. 36, Planets Around Pulsars, ed. J. A. Phillips, S. E. Thorsett, & S. R. Kulkarni (San Francisco, CA: ASP), 149
- Popov, S. B., & Postnov, K. A. 2007, arXiv:0710.2006
- Ravi, V., & Lasky, P. D. 2014, MNRAS, 441, 2433
- Ravi, V., Shannon, R. M., & Jameson, A. 2015, ApJL, 799, L5
- Ruderman, M. A., & Sutherland, P. G. 1975, ApJ, 196, 51
- Shannon, R. M., Cordes, J. M., Metcalfe, T. S., et al. 2013, ApJ, 766, 5
- Spitler, L. G., Cordes, J. M., Hessels, J. W. T., et al. 2014, ApJ, 790, 101
- Tademaru, E. 1971, Ap&SS, 12, 193
- Takata, J., Shibata, S., Hirovani, K., & Chang, H.-K. 2006, MNRAS, 366, 1310
- Thornton, D., Stappers, B., Bailes, M., et al. 2013, Science, 341, 53
- Timmes, F. X., Woosley, S. E., & Weaver, T. A. 1996, ApJ, 457, 834
- Totani, T. 2013, PASJ, 65, L12
- Tremaine, S., & Zytkow, A. N. 1986, ApJ, 301, 155
- Wolszczan, A., & Frail, D. A. 1992, Nature, 355, 145
- Yi, S.-X., Gao, H., & Zhang, B. 2014, ApJL, 792, L21
- Zhang, B. 2014, ApJL, 780, L21